

# Strong Disorder Fixed Point in the Dissipative Random Transverse Field Ising Model

Grégory Schehr

*Theoretische Physik Universität des Saarlandes 66041 Saarbrücken Germany*

Heiko Rieger

*Theoretische Physik, Universität des Saarlandes, 66041 Saarbrücken, Germany*

(Dated: February 8, 2020)

The interplay between disorder, quantum fluctuations and dissipation is studied in the random transverse Ising chain coupled to a dissipative Ohmic bath with a real space renormalization group. A typically very large length scale,  $L^*$ , is identified above which the physics of frozen clusters dominates. Below  $L^*$  a strong disorder fixed point determines scaling at a pseudo-critical point. In a Griffiths-McCoy region frozen clusters produce already a finite magnetization resulting in a classical low temperature behavior of the susceptibility and specific heat. These override the confluent singularities that are characterized by a continuously varying exponent  $z$  and are visible above a temperature  $T^* \sim L^{*-z}$ .

PACS numbers: 75.10.Nr, 75.40.-s, 05.30.Jp, 05.10.Cc

The presence of quenched disorder in a quantum mechanical system may have drastic effects in particular close to and at a quantum critical point. The appearance of Griffiths-McCoy singularities [1, 2], leading to the divergence of various quantities like the susceptibility at zero temperature even far away from a quantum critical point, has received considerable attention recently [3, 4, 5, 6, 7]. This quantum Griffiths behavior is characteristic for quantum phase transitions described by an infinite randomness fixed point (IRFP) [8], which was shown to be relevant for many disordered quantum systems [9].

Quantum Griffiths behavior was proposed to be the physical mechanism responsible for the “non-Fermi-liquid” behavior observed in many heavy-fermion materials [10, 11]. However, it was also argued that in a dissipative environment, as in metals due to the conduction electrons, such a quantum Griffiths behavior might essentially be non-existent [12, 13]. Moreover, even the underlying sharp quantum phase transition itself was shown to be rounded in dissipative model systems [14]. Obviously there is a need to examine carefully the effect of dissipation on a quantum system displaying IRFP and quantum Griffiths behavior in the non-dissipative case and to treat correctly the mixing of critical and Griffiths-McCoy singularities — which is what we intend to do in this letter.

The properties of a single spin coupled to a dissipative bath has been extensively examined [15]. Upon increasing the coupling strength between spin and bath degrees of freedom it displays at zero temperature a transition from a non-localized phase, in which the spin can still tunnel, to a localized phase, in which tunneling ceases and the spin behaves classically. Such a transition is also present in an infinite ferromagnetic spin chain coupled to a dissipative bath, as it was recently shown numerically [16]. Here we want to focus on the interplay of disorder, quantum fluctuations and dissipation and study the Random Transverse Field Ising Chain (RTIC) where each spin is coupled to an ohmic bath of harmonic oscillators [17]. It is defined on a chain of length  $L$  with periodic boundary conditions (p.b.c.) and described by the Hamiltonian  $H$ :

$$H = \sum_{i=1}^L \left[ -J_i \sigma_i^z \sigma_{i+1}^z - h_i \sigma_i^x + \sum_{k_i} \frac{p_{k_i}^2}{2} + \omega_{k_i} \frac{x_{k_i}^2}{2} + C_{k_i, x_{k_i}} \sigma_i^z \right] \quad (1)$$

where  $\sigma_i^{x,z}$  are Pauli matrices and the masses of the oscillators are set to one. The quenched random bonds  $J_i$  (respectively random transverse field  $h_i$ ) are uniformly distributed between 0 and  $J_0$  (respectively between 0 and  $h_0$ ). The properties of the bath are specified by its spectral function  $J_i(\omega) = \frac{\pi}{2} \sum_{k_i} C_{k_i}^2 / \omega_{k_i} \delta(\omega - \omega_{k_i}) = \frac{\pi}{2} \alpha_i \omega e^{-\omega/\Omega_i}$  where  $\Omega_i$  is a cutoff frequency. Initially the spin-bath couplings and cut-off frequencies are site-independent, *i.e.*  $\alpha_i = \alpha$  and  $\Omega_i = \Omega$ , but both become site-dependent under renormalization.

To characterize the ground state properties of this system (1), we follow the idea of a real space renormalization group (RG) procedure introduced in Ref. [18] and pushed further in the context of the RTIC without dissipation in Ref. [3]. The strategy is to find the largest coupling in the chain, either a transverse field or a bond, compute the ground state of the associated part of the Hamiltonian and treat the remaining couplings in perturbation theory. The bath degrees of freedom are dealt with in the spirit of the “adiabatic renormalization” introduced in the context of the (single) spin-boson (SB) model [15], where it describes accurately its critical behavior [19].

Suppose that the largest coupling in the chain is a transverse field, say  $h_2$ . Before we treat the coupling of site 2 to the rest of the system  $-J_1 \sigma_1^z \sigma_2^z - J_2 \sigma_2^z \sigma_3^z$  perturbatively as in [3] we consider the effect of the part  $-h_2 \sigma_2^x + \sum_k (p_k^2/2 + \omega_k x_k^2/2 + C_{k, x_k} \sigma_2^z)$  of the Hamiltonian, which represents a single SB model. For this we integrate out frequencies  $\omega_k$  that are much larger than a lower cut-off frequency  $ph_2 \ll \Omega_2$  with the dimensionless parameter  $p \gg 1$ . Since for those oscillators  $\omega_k \gg h_2$  one can assume that they adjust instantaneously to the current value of  $\sigma_2^z$  the renormalized energy splitting is easily calculated within the adiabatic approximation [15] and one gets an effective transverse field  $\tilde{h}_2 < h_2$ :

$$\tilde{h}_2 = h_2 (ph_2/\Omega_2)^{\alpha_2} \quad , \quad \tilde{\Omega}_2 = ph_2 \quad . \quad (2)$$

If  $\tilde{h}_2$  is still the largest coupling in the chain the iteration (2) is repeated. Two situations may occur depending on the value of  $\alpha_2$ . If  $\alpha_2 < 1$  this procedure (2) will converge to a finite value  $h_2^* = h_2(ph_2/\Omega_2)^{\alpha_2/(1-\alpha_2)}$  and the SB system at site 2 is in a delocalized phase in which the spin and the bath can be considered as being decoupled (formally  $\alpha_2 = 0$ ), as demonstrated by an RG treatment in [19].

If this value  $h_2^*$  is still the largest coupling in the chain it will be aligned with the transverse field. As in the RTIC without dissipation, this spin is then decimated (as it will not contribute to the magnetic susceptibility) and gives rise, in second order degenerate perturbation theory, to an effective coupling  $\tilde{J}_1$  between the neighboring moments at site 1 and 3 [3]

$$\tilde{J}_1 = J_1 J_2 / h_2^* \quad (3)$$

If  $\alpha_2 > 1$ ,  $\tilde{h}_2$  can be made arbitrarily small by repeating the procedure (2) implying that the SB system on site 2 is in its localized phase [19] and essentially behaves classically: the decimation rule (2) indeed amounts to set  $\tilde{h}_2 = 0$ . Such a moment, or cluster of spins, will be aligned with an infinitesimal external longitudinal field and is denoted as ‘‘frozen’’.

Suppose now that the largest coupling in the chain is a bond, say  $J_2$ . The part of the Hamiltonian that we focus on is  $-J_2 \sigma_2^z \sigma_3^z + \sum_{i=2,3} \sum_{k_i} (p_{k_i}^2/2 + \omega_{k_i} x_{k_i}^2/2 + C_{k_i} x_{k_i} \sigma_i^z)$ , i.e a subsystem of two spin-bosons coupled via  $J_2$ . We find that in second order perturbation theory the ground state of this subsystem is equivalent to a single SB system coupled to both baths leading to the additive rule

$$\tilde{\alpha}_2 = \alpha_2 + \alpha_3 \quad (4)$$

Integrating out the degrees of freedom of both baths with frequencies larger than  $pJ_2$  (as done previously for the single SB system [19]) the two moments at 2 and 3 are replaced by a single moment  $\tilde{\mu}_2$  with an effective transverse field  $\tilde{h}_2$ :

$$\tilde{h}_2 = \frac{h_2 h_3}{J_2} \left( \frac{pJ_2}{\Omega_2} \right)^{\alpha_2} \left( \frac{pJ_2}{\Omega_3} \right)^{\alpha_3} \quad (5)$$

$$\tilde{\mu}_2 = \mu_2 + \mu_3 \quad , \quad \tilde{\Omega}_2 = pJ_2 \quad (6)$$

where  $\mu_i$  is the magnetic moment of site  $i$  (in the original model, one has  $\mu_i = 1$  independently of  $i$ ). Combining Eq. (4) and Eq. (6) one clearly sees that  $\tilde{\alpha}_i = \tilde{\mu}_i \alpha$ .

In the following we analyze this RG procedure defined by the decimation rules (2-6) numerically. This is done by considering a finite chain of size  $L$  with p.b.c. and iterating the decimation rules until only one site is left. This numerical implementation has been widely used in previous works [9], and it has been shown in particular to reproduce with good accuracy the exact results of Ref. [3] for the RTIC. We fix  $h_0 = 1$  and concentrate on the parameter plane  $(\alpha, J_0)$ . All data were obtained by averaging over  $10^5$  different disorder realizations (if not mentioned otherwise), and the disorder average of an observable  $O$  is denoted by  $\bar{O}$ . The decimation rules (2-6) depend explicitly on the ‘‘ad hoc’’ parameter  $p$  (or more precisely on the ratio  $\Omega/p$ ). For the moment we fix  $\Omega/p = 10^4$  and discuss the weak dependence on this parameter below.

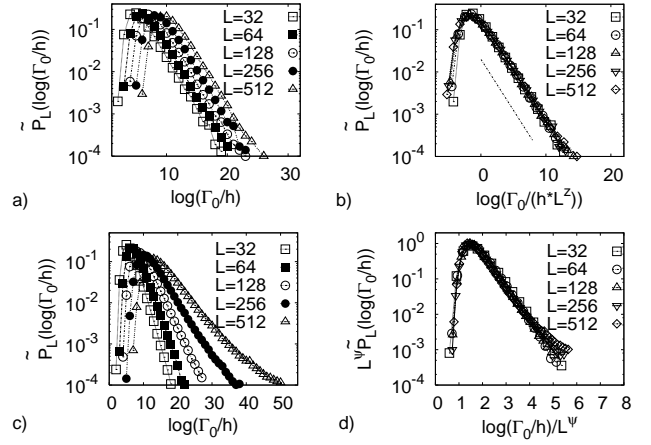


FIG. 1: **a)**  $\tilde{P}_L(\log(\Gamma_0/h))$  as a function of  $\log(\Gamma_0/h)$  for different system sizes  $L$  for  $\alpha = 0.03$  ( $h_0 = 1$ ,  $J_0 = 0.34$ ), i.e. far from the pseudo-critical point. **b)**  $\tilde{P}_L(\log(\Gamma_0/h))$  as a function of  $\log(\Gamma_0/hL^z)$  for different system sizes for  $\alpha = 0.03$  ( $h_0 = 1$ ,  $J_0 = 0.34$ ). The straight dashed line has slope  $1/z$  with  $z = 1.65(5)$ . **c)**  $\tilde{P}_L(\log(\Gamma_0/h))$  as a function of  $\log(\Gamma_0/h)$  for different system sizes  $L$  for  $\alpha = 0.052$  ( $h_0 = 1$ ,  $J_0 = 0.34$ ), i.e. at the pseudo-critical point. **d)**  $L^\psi \tilde{P}_L(\log(\Gamma_0/h))$  as a function of  $\log(\Gamma_0/h)/L^\psi$  for different system sizes for  $\alpha = 0.052$ ,  $\psi = 0.32$ .

The transverse field  $h$  acting on the last remaining spin is an estimate for the smallest excitation energy. Its distribution,  $P_L(h/\Gamma_0)$ , where  $\Gamma_0$  is the largest coupling in the initial chain of size  $L$ , reflects the characteristics of the gap distribution [6]. Since the last spin can either be frozen (i.e the last field  $h$  is zero) or non-frozen we split  $P_L(h/\Gamma_0)$  into two parts:

$$\tilde{P}_L(h/\Gamma_0) = A_L \tilde{P}_L(h/\Gamma_0) + (1 - A_L) \delta(h/\Gamma_0) \quad (7)$$

where  $\tilde{P}_L(h/\Gamma_0)$  is the restricted distribution of the last fields in the samples that are non-frozen and  $A_L$  is the fraction of these samples. It, or equivalently  $\tilde{P}_L(\log(\Gamma_0/h))$ , represents the distribution of the smallest excitation energy in the ensemble of non-localized spins.

Let us first present data obtained for  $J_0 = 0.34$ . Fig. 1a shows  $\tilde{P}_L(\log(\Gamma_0/h))$ , for  $\alpha = 0.03$ . For a system close to, but not at, a quantum critical point described by an IRFP one expects indications of Griffiths-McCoy singularities characterized by the following scaling behavior for  $\tilde{P}_L$

$$\tilde{P}_L(\log(\Gamma_0/h)) = \mathcal{P}(\log(\Gamma_0/hL^z)) \quad (8)$$

where  $z$  is a dynamical exponent continuously varying with  $(J_0, \alpha, \text{etc.})$ . Fig. 1b shows a good data collapse with  $z = 1.65$  for the chosen coupling constant  $\alpha = 0.03$ . The slope of the dotted line in Fig. 1b is identical to  $1/z$  and upon increasing  $\alpha$  we observe that the slope,  $1/z$ , decreases. Our numerical estimates for  $1/z(\alpha)$  are shown in Fig. 2; they indicate that  $1/z$  approaches zero for some critical value  $\alpha_c$ , which implies formally  $z \rightarrow \infty$  for  $\alpha \rightarrow \alpha_c$ . This is also characteristic for an IRFP, where  $\tilde{P}_L(\log(\Gamma_0/h))$  is expected to scale as

$$\tilde{P}_L(\log(\Gamma_0/h)) = L^{-\psi} \mathcal{P}_{\text{IRFP}}(L^{-\psi} \log(\Gamma_0/h)) \quad (9)$$

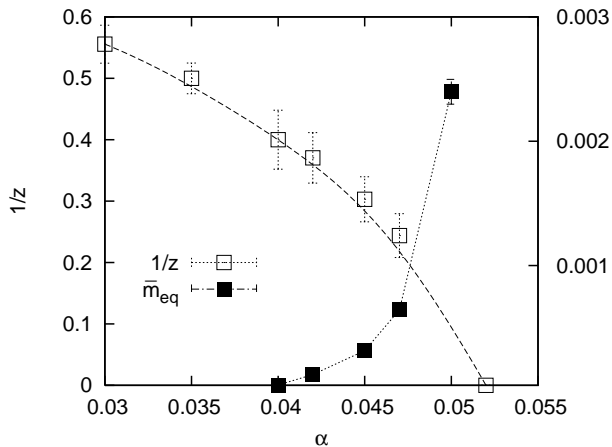


FIG. 2: Magnetization  $\bar{m}_{\text{eq}}$  and inverse dynamical exponent  $1/z$  as a function of  $\alpha$  (for  $h_0 = 1, J_0 = 0.34$ )

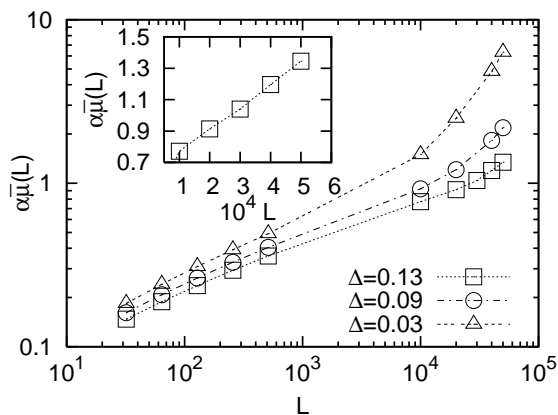


FIG. 3: Magnetic moment  $\alpha\bar{\mu}(L)$  as a function of the system size  $L$  for different values of  $\delta$ . **Inset**:  $\alpha\bar{\mu}(L)$  for  $L \geq 10^4$  as a function of  $L$  and for  $\Delta = 0.13$ . The linear behavior suggests a finite  $\bar{m}_{\text{eq}}$ . The lines are guides to the eyes. Due to the large system sizes the data are averaged only over 500 different disorder realizations.)

$\psi$  is a critical exponent characterizing the IRFP. Fig. 1c shows  $\tilde{P}_L(\log(\Gamma_0/h))$  for  $\alpha = 0.052$ : one observes that it broadens systematically with increasing system size, in contrast to the data shown in Fig. 1a, and Fig. 1d displays a good data collapse according to (9) with  $\psi = 0.32$ . Varying  $\alpha$  only slightly worsens the data collapse substantially, therefore we take  $\alpha_c = 0.052$  as our estimate for the putative critical point (for  $h_0 = 1$  and  $J_0 = 0.34$ ) and denote by  $\Delta = (\alpha_c - \alpha)/\alpha_c$  the distance from it.

The magnetic moment  $\mu$  of the last remaining spin in the decimation procedure represents an estimate of the total magnetization  $\bar{m}_{\text{eq}}L$  of the chain. In Fig. 3, we show  $\alpha\bar{\mu}(L)$  as a function of  $L$  for different values of  $\Delta$ . For small  $L$ ,  $\bar{\mu}(L) \propto L^a$  with  $a \simeq 1/3$  up to a length scale  $L^* \sim O(10^4)$  beyond which the effective coupling between strongly coupled clusters and the bath,  $\alpha\bar{\mu}$ , gets larger than one and the clusters become

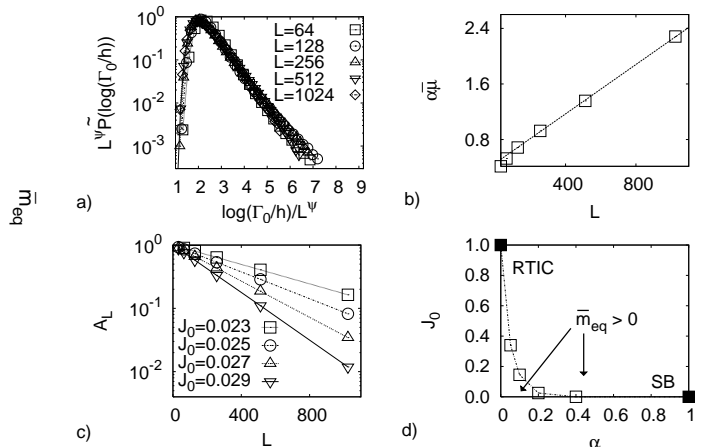


FIG. 4: **a)**  $L^\psi \tilde{P}_L(\log(\Gamma_0/h))$  as a function of  $\log(\Gamma_0/h)/L^\psi$  with  $\psi = 0.31$  for different system sizes for  $\alpha = 0.2$  and  $J_0 = 0.025$ . **b)** Magnetic moment  $\alpha\bar{\mu}(L)$  as a function of the system size  $L$  for  $\alpha = 0.2$  and  $J_0 = 0.025$  suggesting  $\bar{m}_{\text{eq}} > 0$  and  $L^* \sim 100$ . **c)**  $A_L$  as a function of  $L$  on a linear-log plot for different values of  $J_0$  and  $\alpha = 0.2$ . **d)** Phase diagram for  $h_0 = 1$  and  $\Omega/p = 10^4$  characterized by a single phase with  $\bar{m}_{\text{eq}} > 0$ . The dotted line represents the line of smeared transitions characterized by an IRFP scaling (7,9).

localized. Above this value  $\bar{\mu}(L) \sim \bar{m}_{\text{eq}}L$  (see inset of Fig. 3), which suggests a finite magnetization  $\bar{m}_{\text{eq}}$  before the putative critical point is reached. This is a manifestation of the “frozen” clusters and lead to the concept of rounded quantum phase transitions in the presence of dissipation [14]. The typical size of a frozen cluster turns out to be rather large  $L^* \geq 10^4$  for this range of parameters ( $\alpha = 0.03 - 0.052, J_0 = 0.34$ ). Consequently the fraction of non-frozen samples,  $A_L$ , in (7) is close to 1 for the system sizes that we could study numerically.

A stronger dissipation strength  $\alpha$  reduces  $L^*$  and gives us the possibility to study the crossover to a regime that is dominated by frozen clusters, in particular the  $L$ -dependence of  $A_L$  in (7), and we consider  $\alpha = 0.2$  as an example now. For the restricted distribution  $\tilde{P}(\log(\Gamma_0/h))$ , we obtain the same scenario as for smaller dissipation, as shown in Fig. 4a for the putative critical point  $J_{0c} = 0.025$ . Fig. 4b, shows  $\alpha\bar{\mu}(L)$  indicating that  $\bar{\mu}(L) \propto \bar{m}_{\text{eq}}L$  for  $L > 100$ , which implies  $L^* \sim 100$ . The fraction of non-frozen samples,  $A_L$ , shows a clear deviation from unity already for the system sizes we study here: Fig. 4c shows  $A_L$  as a function of  $L$  for different values of  $J_0$ . The data imply an exponential decay  $A_L \propto e^{-L/\tilde{L}}$ . The characteristic decay length fits well to  $\tilde{L} \propto J_0^{\alpha-\beta}$ , with  $\beta \simeq 0.8$ , meaning a very rapid increase of  $\tilde{L}$  with decreasing dissipation strength  $\alpha$ . By comparing  $\tilde{L}$  with  $L^*$  for various parameters  $(\alpha, J_0)$  we find that  $\tilde{L} = \kappa L^*$ , with  $\kappa$  a dimensionless number of order one, weakly dependent on  $\alpha$  and  $J_0$ .

As long as  $L < L^*$  the restricted distribution is not significantly different from the full distribution of non-vanishing excitation energies, since the probability for a frozen sample is small for  $L \ll L^*$ . Since  $\tilde{P}_L$  has a power law tail down to excitation energies exponentially small in  $L$ , the spe-

cific heat, susceptibility etc. in finite size systems display a singular low temperature behavior characterized by the dynamical exponent  $z(\alpha)$  down to very low temperatures (actually down to  $T_L \sim e^{-aL}$ ). This intermittent singular behavior,  $\chi(T) \sim T^{-1+1/z(\alpha)}$  for the susceptibility and  $c(T) \sim T^{1/z(\alpha)}$  for the specific heat, persists for larger system sizes as well as for  $L \rightarrow \infty$ , but as soon as  $L > L^*$  it will eventually compete with the temperature dependence of the (quantum mechanically) frozen clusters - e.g.  $1/T$  for the susceptibility. Since the latter has a small amplitude proportional to  $1/L^*$ , classical temperature dependence will only set in below  $T^* \sim L^{*-z(\alpha)}$  and Griffiths-like behavior is visible (also in the infinite system) above  $T^*$ .

It is instructive to consider the RTIC without dissipation, but with a finite fraction  $\rho$  of zero transverse fields (i.e.  $p(h) = \rho\delta(h) + h_0^{-1}(1-\rho)\theta(h)\theta(h_0-h)$ ). The sites with  $h=0$  then correspond to frozen clusters that have an average distance  $L^* \propto \rho^{-1}$ . Indeed the distribution  $P(h/\Gamma_0)$  shows the same behavior as in Eq. (7) with  $A_L \sim e^{-L/L^*}$ . But, in contrast to the dissipative case, the restricted distribution  $\tilde{P}(\log(\Gamma_0/h))$  is naturally identical with the one for the non-diluted ( $\rho=0$ ) RTIC, which shows the IRFP scaling (9) at  $h_0 = J_0$  with  $\Psi_{\text{RTIC}} = 0.5$ , different from the one we obtain here.

The connected correlation function  $\bar{C}(r) = \langle \sigma_i^z \sigma_{i+r}^z \rangle - \langle \sigma_i^z \rangle \langle \sigma_{i+r}^z \rangle$  decays exponentially for  $r \gg L^*$ , given that the quantum fluctuations are exponentially suppressed beyond this length scale (7), consistent with [14]. It should also be noted that the connected correlation function of the restricted ensemble of non-frozen samples  $\bar{C}(r)$  does not behave critically since the number of non frozen spins belonging to the same cluster is bounded by  $1/\alpha$  in the restricted ensemble. Thus, the origin of the systematic broadening of the distribution  $\tilde{P}(\log \Gamma_0/h)$  is here different from a standard IRFP and probably stems from the non-localized clusters with  $\alpha_i$  close to (but smaller than) one (see Eq. 2).

We have checked that the behavior of the gap distribution characterized by Eq. (7,9) depends very weakly on the *ad hoc* parameter  $\Omega/p$  in the range  $10 - 10^4$ . In this range, the relative variations of the estimated exponent  $\psi$  is of the order of 5%, although the values of  $L^*$  and  $(\alpha_c, J_{0c})$  are more sensitive, and probably non universal. We repeated the previous analysis for different values of  $(\alpha, J_0)$  (keeping  $h_0 = 1$ ). In contrast to the pure case [16], the entire plane is here characterized by a single phase where  $\bar{m}_{\text{eq}} > 0$ , beyond a length scale  $L^* \equiv L^*(\alpha, J_0)$ , everywhere (except on the boundaries  $(\alpha, 0)$  and  $(0, J_0)$ ) [20]. One can identify a line of smeared transitions associated with the broadening of the restricted gap distribution  $\tilde{P}(\log(\Gamma_0/h))$ , according to (9): this is depicted in Fig. 4d. We find that the associated exponent  $\psi$  vary weakly along this line, its relative variation being less than 10%.

To conclude our strong disorder RG study of the RTIC coupled to a dissipative Ohmic bath revealed that non-frozen samples display an IRFP scaling of the distribution of excitation energies. With this we computed a continuously varying exponent  $z(\alpha)$  that determines an intermittent singular temperature dependence of thermodynamic quantities above a temper-

ature  $T^* \sim L^{*-z(\alpha)}$ .  $L^*$  is a characteristic length scale above which the ground state displays a non-vanishing magnetization, as predicted by the smeared transition scenario [14], and that we determined to increase exponentially with the inverse strength of the dissipative coupling. This implies that numerical studies can hardly track the asymptotic behavior [17] and that experiments at very low but non-vanishing temperatures might still show indications for quantum Griffiths behavior [10, 12, 13]. In higher dimensions we expect a similar scenario as the one discussed here and it would be interesting to extend our study to Heisenberg antiferromagnets and XY systems.

HR thanks the Aspen Center for Physics, where parts of this work were done, for its kind hospitality, and T. Vojta for stimulating discussions. GS acknowledges the financial support provided through the European Community's Human Potential Program under contract HPRN-CT-2002-00307, DYGLAGEMEM.

- 
- [1] R. B. Griffiths, Phys. Rev. Lett. **23**, 17 (1969).
  - [2] B. M. McCoy, Phys. Rev. Lett. **23**, 383 (1969); Phys. Rev. **188**, 1014 (1969).
  - [3] D. S. Fisher, Phys. Rev. Lett. **69**, 534 (1992); Phys. Rev. B **51**, 6411 (1995).
  - [4] M. J. Thill and D. A. Huse, Physica A **214**, 321 (1995).
  - [5] H. Rieger and A. P. Young, Phys. Rev. B **54**, 3328 (1996); M. Guo, R. N. Bhatt and D. A. Huse, Phys. Rev. B **54**, 3336 (1996).
  - [6] F. Iglói and H. Rieger, Phys. Rev. B **57**, 11404 (1998).
  - [7] C. Pich, A. P. Young, H. Rieger, and N. Kawashima, Phys. Rev. Lett. **81**, 5916 (1998).
  - [8] D. Fisher, Physica A **263**, 222 (1999); O. Motrunich, S.-C. Mau, D. A. Huse, and D. S. Fisher, Phys. Rev. B **61**, 1160 (2000).
  - [9] For a recent review, see F. Iglói and C. Monthus, Phys. Rep. **412**, 277 (2005).
  - [10] M. C. deAndrade et al., Phys. Rev. Lett. **81**, 5620 (1998); A. H. Castro Neto, G. Castilla, and B. A. Jones, Phys. Rev. Lett. **81**, 3531 (1998).
  - [11] G. R. Stewart, Rev. Mod. Phys. **73**, 797 (2001).
  - [12] A. H. Castro Neto and B. A. Jones, Phys. Rev. B **62**, 14975 (2000); Europhys. Lett. **71**, 790 (2005).
  - [13] A. J. Millis, D. K. Morr, and J. Schmalian, Phys. Rev. Lett. **87**, 167202 (2001); Phys. Rev. B **66**, 174433 (2002).
  - [14] T. Vojta, Phys. Rev. Lett. **90**, 107202 (2003).
  - [15] A. Legget *et al.*, Rev. Mod. Phys., **59**, 1 (1987).
  - [16] P. Werner, K. Völker, M. Troyer, and S. Chakravarty, Phys. Rev. Lett. **94**, 047201 (2005).
  - [17] L. F. Cugliandolo, G. S. Lozano, and H. Lozza, Phys. Rev. B **71**, 224421 (2005).
  - [18] S.K.Ma, C. Dasgupta and C.K. Hu, Phys. Rev. Lett. **43**, 1434 (1979); C.Dasgupta and S.K. Ma, Phys. Rev. B **22**, 1305 (1980).
  - [19] R. Bulla, H.-J. Lee, N.-H. Tong, and M. Vojta, Phys. Rev. B **71**, 045122 (2005).
  - [20] Computing the dependence of  $\bar{m}_{\text{eq}}$  as a function of the distance from the pure critical point [14] requires a precise estimate of the critical line itself, which is not feasible with our method.